Preprint
UCRL-JC-136785

Laser-Plasma Interaction Physics at LULI

C. Labaune, J. Fuchs, S. Depierreux, A. Michard, H.A. Baldis, D. Pesme, G. Laval and S. Hüller

This article was submitted to
Ist International Conference on Inertial Fusion Sciences and Applications
Bordeaux, France
September 12-17, 1999

December 8, 1999

U.S. Department of Energy

Lawrence
Livermore
National
Laboratory

UCRL-JC-136785

Laser-plasma interaction physics at LULI

C. Labaune[1], J. Fuchs[1], S. Depierreux[1], A. Michard[1]
H.A. Baldis[2]
D. Pesme[3], G. Laval[3], S. Hüller[3]

[1]*Laboratoire pour l'Utilisation des Lasers Intenses, Ecole Polytechnique, Centre National de la Recherche Scientifique, 91128 Palaiseau cedex, France*
[2]*Institute for Laser Science and Applications (ILSA) Lawrence Livermore National Laboratory, POB 808, Livermore CA 94550, USA*
[3]*Centre de Physique Théorique, Ecole Polytechnique, Centre National de la Recherche Scientifique, 91128 Palaiseau cedex, France*

Abstract

Laser-plasma interaction physics is studied in the context of laser fusion using the six-beam laser facility at LULI. Interaction between RPP laser beams and well-characterized preformed plasmas has been performed to study various aspects of stimulated Brillouin and Raman scattering (SBS and SRS), self-focusing and filamentation. Thomson scattering of a short wavelength probe laser beam was used to provide a complete characterization of the plasma (electron temperature, density, flow velocity) and measurements of the density fluctuations associated with ion acoustic waves and electron plasma waves, with temporal, spatial, frequency and wavenumber resolution. Among the different studies, we will present results on the effect of polarization smoothing, target material, multi-species plasmas, and Langmuir decay on parametric instabilities.

1. Introduction

The coupling of intense laser beams with plasmas has important implications for inertial confinement fusion (ICF) [1]. Of particular relevance are scattering instabilities, stimulated Brillouin and Raman scattering (SBS and SRS), filamentation and self-focusing of the laser light. These instabilities can reduce the laser-plasma coupling efficiency, produce very energetics electrons which can preheat the fusion fuel and reduce the compression rate, and modify the intensity distribution, affecting the uniformity of energy deposition [2,3].

In the direct drive approach to ICF, the capsule is directly irradiated by a large number of symmetrically arranged laser beams. The propagation of the laser beams through the underdense plasma surrounding the target and the interaction mechanisms determine the energy deposition performance and uniformity. The underdense plasma is the region of plasma with electron density n_e $n_c = 1.1 \times 10^{21} / \lambda_{\mu m}^2$ (cm^{-3}) , where n_c is the critical density for the laser wavelength λ. To achieve high gain, a good control of parametric instabilities is needed.

In the indirect drive approach, multiple laser beams irradiate a cylindrical radiation enclosure (hohlraum). The laser energy is converted into x-rays inside the hohlraum, which in turn irradiate the capsule containing the fuel. This scheme has the advantage of being less sensitive to small-scale non-uniformities of the laser beams. Conversely, a potential disadvantage is the presence of a large scale length of plasma traversed by the laser inside the hohlraum, that can grow parametric instabilities. This plasma is produced by irradiation of a low-Z gas filling the hohlraum to inhibit motion of the laser absorption and X-ray emission region and to prevent early axial stagnation of the high-Z plasma blow-off. A particular issue, in this scheme, is the influence of the high-Z plasma near the hohlraum wall in the generation of SBS.

In both direct and indirect drive schemes, as the laser wave propagates through the underdense plasma, the light can decay into a combination of scattered electromagnetic waves (EMW), and local longitudinal modes of the plasma. In the absence of magnetic fields, a plasma can sustain electromagnetic waves and two plasma modes : ion acoustic waves (IAW), and electron plasma waves (EPW). Even if the plasma may have strong self-generated magnetic fields, IAW and EPW are the only modes of importance in these plasmas [4].

The decay of the incident EMW (laser light) into local modes (either IAW or EPW) and a scattered EMW, enhances the level of density fluctuations $(\frac{\delta n}{n})_{IAW,EPW}$ associated with the local mode, due to the ponderomotive force generated by the beating between the two EMW [5]. This increase of $(\frac{\delta n}{n})_{IAW,EPW}$ further enhances the decay, thus generating a feed-back loop that leads to unstable growth, and thus to the creation of an instability. If the waves involved in the decay satisfies conservation of energy, $\omega_0=\omega_1+\omega_2$, and conservation of momentum, $k_0=k_1+k_2$ (where 1 is the scattered EMW, 2 is either an IAW or an EPW, and ω and k are the respective frequency and wavevector for each wave) the decay grows exponentially. This exponential growth is certainly a potential problem in ICF : the scattered EMW can leave the plasma, thus loosing a large fraction of the laser energy, as well as producing a redistribution of the laser energy inside the hohlraum, affecting the requirements for symmetry of implosion. The instabilities of interest are stimulated Brillouin scattering (SBS), and stimulated Raman scattering (SRS). Stimulated Brillouin scattering consists of the decay of the incident EM wave into a scattered EMW and an IAW, and stimulated Raman scattering consists of the decay of the incident EMW into a scattered EMW and an EPW.

Self-focusing and filamentation are triggered by laser intensity modulations in the focal spot and grow due to the refractive index changes caused by either thermal or ponderomotive effects. This results in an increase of intensity and an eventual beam breakup. Filamentation can have detrimental consequences to the hydrodynamics of an ICF plasma, as well as affect the growth of parametric instabilities, adding to the complexity of the study of SBS and SRS.

Of vital importance for ICF are the understanding and control of parametric instabilities at a low level. Understanding of the behavior of the instabilities in present targets is needed to extrapolate with confidence the actual measurements to the plasma and laser parameters of the future megajoule experiments. Among the actual objectives is the understanding of the saturation mechanisms, involving non linear effects and secondary decays. One important difficulty is the coupling between instabilities. The growth of instabilities is modified by the presence of waves

(either IAW or EPW) associated with other instabilities, or in the presence of waves associated with secondary decays such as the parametric decay of the EPW from SRS. A further complication arises when considering the overlap of multiple laser beams. Not only is there the interplay between instabilities driven by one beam, but also the interplay between instabilities driven by different beams. Waves associated with different parametric decays can interact among themselves, modifying in turn the behavior of the instabilities. Transfer of energy between crossing beams through parametric processes can destroy the initial energy balance and affect local beam intensity with consequence on local instability gain [6,7].

Control of filamentation, SBS and SRS is expected to be possible by temporal and spatial smoothing of the laser beam intensity distribution [8]. The simplest spatial smoothing technique consist of a random phase plate (RPP) which is placed in front of the focusing optics and which breaks the wave front into many beamlets, each being randomly dephased by 0 or π [9]. The far-field intensity distribution consists of an overall envelope determined by an individual phase plate element. Within this envelope there is a stationnary fine-scale speckle structure due to the interferences between different phase element contributions, whose dimensions are determined by the f/number of the focusing optics. This focusing system almost eliminates the initial phase and amplitude defaults of the laser beam and create a well-characterized laser focal spot that is nearly independent of the particular aberrations of the laser system. Temporal smoothing of the previous distribution can be obtained by spectral dispersion (SSD) which rapidly varies in time the fine-scale speckle structure [10]. The laser pulse is spectrally broadened by FM phase modulations and is angularly dispersed by a diffraction grating. The resulting focal spot consists of the superposition of many RPP smoothed electromagnetic field patterns associated with each frequency component of the laser. As a result of the diffraction grating, these patterns are sligthly offset spatially from each other. This kind of smoothing can limit the time available for growth of the parametric instabilities by moving the high-intensity speckles before the instabilities have time to grow. In addition to the previous techniques, polarization smoothing consists in dividing the light power into two crossed polarizations with slightly different angular directions [11,13]. This is obtained by propagating the linearly polarized laser beam through a wedged birefringent crystal with its two axis at 45° from the polarization. This technique reduces the intensity contrast of the focal spot pattern and the number of high intensity speckles which are the ones which contribute the most to parametric instabilities.

Another way to limit the growth of parametric instabilities is to increase the damping of one of the daughters waves. For example, increasing the ion wave damping reduces the SBS growth as observed in experiments using multi species ions [14,16]. The surprising result in these experiments was the increase of SRS with increased ion wave damping which need to invoke some dependence of SRS on ion acoustic waves. This could be due to the Langmuir decay instability (LDI) where the primary EPW produced by SRS can decay into an IAW and a secondary EPW. Although secondary EPW have been observed, some alternative explanations were proposed [17]. LDI is very important as it could produce non linear saturation of the Raman instability [18].

In this paper, we will present results from a multiple beam experiment achieved at LULI (Laboratoire pour l'Utilisation des Lasers Intenses) where the principal parametric instabilities

produced by the interaction of a 1.053 μm laser beam and a preformed plasma were studied by means of Thomson scattering. Three studies are presented : 1) effect of the plasma composition on SBS and SRS reflectivities ; 2) effect of polarization smoothing on interaction mechanisms ; 3) demonstration of the occurence of the Langmuir decay instability based on the simultaneous observation of the two products of the instability.

2. Experimental set-up and diagnostics

The laser beam configuration and geometry of the Thomson scattering diagnostic are shown in Fig. 1. The 600ps FWHM Gaussian beams were all in the horizontal plane and arrived at the target at different times. The plasma forming and the heating beams were as follows : two 0.53μm plasma producing beams at t=0 and two 0.53μm plasma heating beams at t=0.5 ns. The 0.35μm Thomson scattering probe beam and the 1.05μm interaction beam were synchronous and were set-up at three different times : t=1 ns, t=1.4 ns, t=1.8 ns to explore the effect of the plasma density. Random phase plates (RPP) were used on all the beams to provide reproducible conditions from shot to shot and well-characterized intensity distributions in the focal volumes. The interaction beam was focused along the axis of symmetry of the plasma with an f/6 lens through an RPP of 2mm square elements. The resulting focal spot diameter was 320 μm full width at half maximum (FWHM), producing a peak average intensity of 10^{14} W/cm^2.

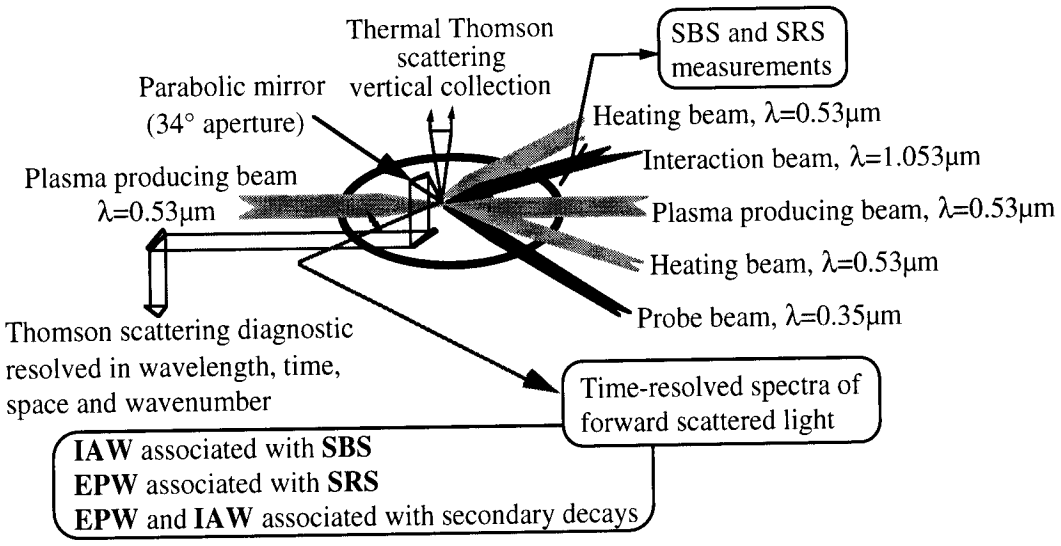

Figure 1 : Experimental set-up of the LULI experiment showing the beam configuration and the principal diagnostics

The 351 nm-wavelength Thomson scattering probe was focused with a combination of a lens and an RPP with elongated elements, to form a focal region 100 μm by 1 mm along the axis of the interaction beam, thus allowing to probe scattered light off the plasma waves over the whole interaction length. The Thomson scattered light was collected by a parabolic mirror and imaged onto three spectrometer-streak camera combinations by secondary spherical mirrors. Two positions were used for the parabolic mirror to collect scattered light off primary and secondary IAW and EPW associated with SBS and SRS occuring preferentially in the backward direction. Masks were used as required, to select the waves of interest at different stages during the experiment. Multiple slits were used on the streak cameras to record simultaneously light scattered from different regions of plasma along the laser axis [19]. This diagnostic provides time, space, wavenumber and frequency resolved measurements of the intensity of the density fluctuations associated with the primary and secondary plasma waves pumped by the interaction beam. Absolute measurements of SBS and SRS reflectivities and SBS time-resolved spectra of the light collected by the focusing lens of interaction beam ($\delta\omega$=0.045 sr) were accomplished, providing

complementary measurements on the elecromagnetic waves produced by the SBS and SRS decays. Light emitted in the forward direction of the interaction beam was spectrally analysed with angular resolution.

3. Plasma characterization

The targets were thin micro-disks of 400 μm diameter of CH, Al, C, Au and mixed C/Au. A careful choice of the initial target thicknesses and time delays between the plasma producing beams and the interaction beam assured that all the target material has been ablated at the time of interaction, and that the plasma has expanded to the desired electron density. The target thickness was 1.2, 0.5, 0.5, 0.12 and 0.3 μm for CH, Al, C, Au and mixed C(80%)/Au(20%), respectively. Most of the results presented in this paper, apart from §4, are for CH targets. Plasma density and temperature were characterized using both thermal and enhanced Thomson scattering spectra. Thermal Thomson scattered light was recorded in the vertical direction,with an f/1 lens, where there is no contribution from pumped waves by the interaction beam. Typical dimensions of the probed volumes were 40 μm along the interaction axis, 30 μm in height and 100 μm in the remaining direction. The time-resolved spectra provided electron temperature and expansion velocity during the interaction pulse. Figure 2 shows the electron temperature and the velocity profiles at the beginning of the interaction pulse. The electron temperature was around (0.7±0.1) keV and constant along the laser axis direction. The temporal evolution of the electron density at specific locations in the plasma and the electron density profiles along the laser axis during the interaction pulse were inferred using Thomson scattered spectra off EPWs associated with SRS and recorded simultaneously at different places in the plasma. The electron density at the peak of the plasma profile evolves from $(0.3\pm0.025)xn_c$ to $(0.05\pm0.01)xn_c$ from the beginning to the end of the interaction beam (where $n_c = 1.1x10^{21}$ cm^{-3} is the critical electron density for $\lambda = 1.053$ μm light). The typical scalelength of the parabolic profile of the plasma was 500 μm at the peak of the interaction pulse.

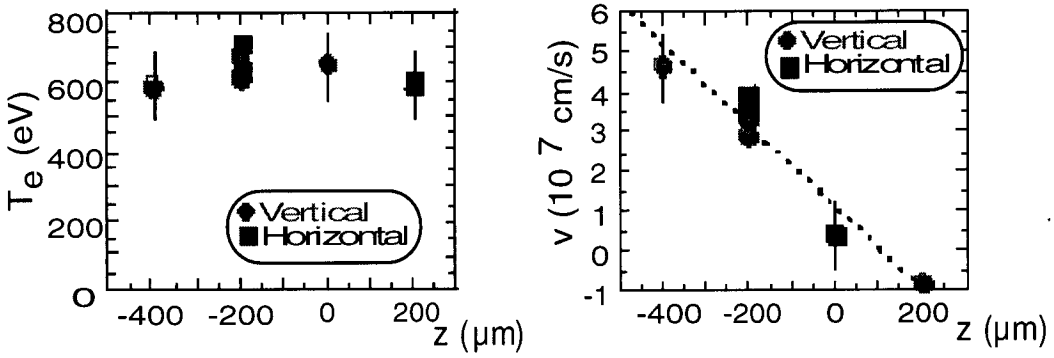

Figure 2 : Temperature and velocity profiles along the interaction beam axis in CH plasmas as measured from thermal Thomson scattered spectra recorded in the vertical and in the horizontal directions. z=0 corresponds to the summit of the density profile.

4. Effect of the target composition on stimulated Brillouin and Raman scattering

We observed a clear dependence of the SBS and SRS reflectivities on the target composition as shown in Fig.3. These data have been obtained for a time delay of 1ns between the interaction beam and the plasma producing beams. Both SBS and SRS reflectivities are higher for the mixing of either CH, or C/Au, as compared with pure Au, Al and C. This effect is particularly pronounced for SRS, for which significative levels of SRS are observed only with the mixed targets. Both SBS and SRS from carbon are very weak.

For all targets, the SBS reflectivity decreases with the time delay of the interaction beam. As the electron temperature was mainly determined by heating by the interaction beam, increasing the time delay principally corresponds to a decrease of the overall electron density. The observed SBS behavior is in agreement with what is predicted by linear theory that SBS increases with electron density. It is opposite to what has been observed in other experiments [16]. For SRS, we observed a maximum of reflectivity for the short time delays, 1 or 1.4 ns. This is probably due to the fact that the electron density is more favorable for SRS growth at that time.

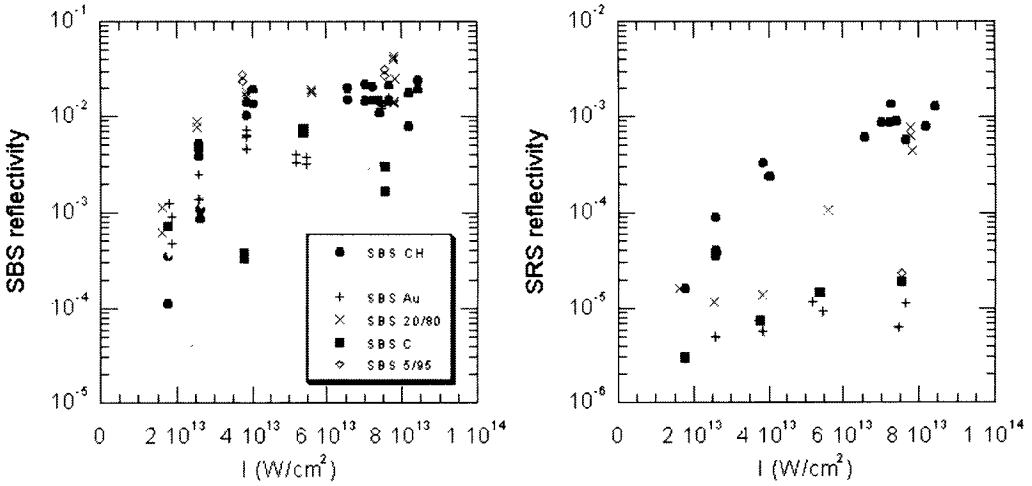

Figure 3 : SBS and SRS reflectivities measured in backward direction as a function of laser intensity for different target composition.

Significative differences between the targets have been observed on the SBS spectra. They are almost completely blue shifted in the case of CH and Al targets, and almost completely red shifted for Au, C and C/Au targets. These shifts are in agreement with the Doppler shift predicted by the measurements of the location of the IAW in the velocity profile, with Thomson scattering. The SBS shifts are a strong indication that SBS may be happening in different regimes depending on the target composition. One of the most likely explanation of the blue shift is the occurence of filamentation of the laser beam after propagating a short distance in the plasma. Spreading of the light at the output of the filament can lead to a decrease of the laser intensity at higher densities in the profile and consequently to a reduction of SBS. The differences in the SBS spectra could be an indication that filamentation instability is not the same in the different plasmas. Interpretation of the results is not straightforward and need complete simulations including SBS, SRS, filamentation and the modification of the ion acoustic damping with multi species ions.

5. Effect of polarization smoothing on parametric instabilities

By adding polarization smoothing (PS) to the RPP, we have observed significative reduction of the levels of the density fluctuations associated with the plasma waves, as well as SBS and SRS reflectivities. Complete reflectivity measurements are presented in another paper of this book and show a typical reduction of the backscattered light by a factor 10 for SBS and by a factor 3 for SRS. Forward scattering was also affected by polarization smoothing. The time-resolved spectra of the light propagating in the forward direction outside the cone of the focusing lens exhibit two

components on which the red-shifted component with respect to the initial laser wavelength is reduced in presence of PS, as shown in Figure 4. This red-shifted component is interpreted as scattering of the laser light on ion acoustic waves which can be produced by forward Brillouin scattering or plasma induced smoothing. These results show that these IAW are reduced by PS.

PS is mainly affecting the laser intensity disribution in the focal volume. The probability law which describes the speckle distribution in the focal spot of an RPP beam is modified from $P(I) = (1/I_0)\, e^{-I/I_0}$ to $P_{PS}(I) = (4\, I/I_0^2)\, e^{-2I/I_0}$ when PS is added. The intensity contrast, $C = \sqrt{(\langle I^2\rangle - \langle I\rangle^2)/\langle I^2\rangle}$, is then reduced from 1 to $1/\sqrt{2}$. The fraction of the beam intensity above nI_0 (I_0 being the averaged peak intensity) goes from $(1+n)\exp(-n)$ for RPP to $(1+2n+2n^2)\exp(-2n)$ for PS, indicating that the fraction of the laser power in the high intensity speckles is reduced. As the most intense speckles are those leading to strong self-focusing and growth of SRS and SBS, their reduction can explain the decrease of parametric instabilities with PS [20,21].

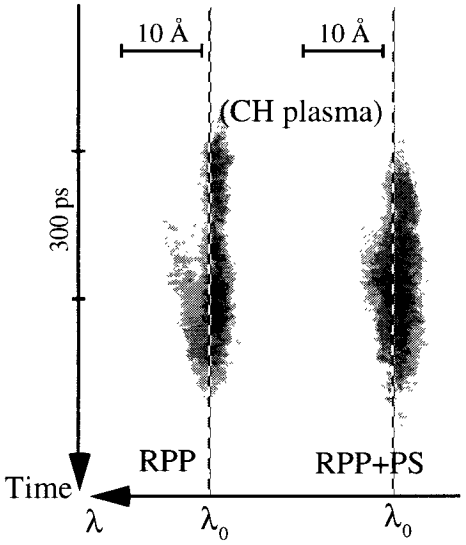

Figure 4 : Time-resolved spectra of forward scattered light outside the focusing cone with RPP and RPP+PS. The laser intensity is 8×10^{13} W/cm².

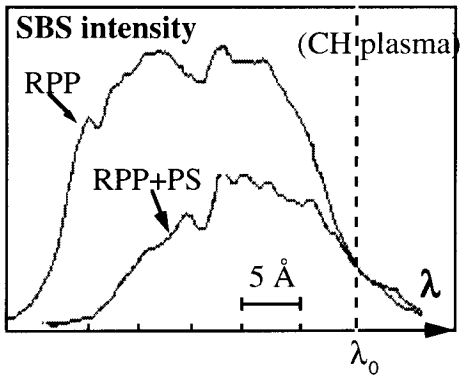

Figure 5 : Comparison of the SBS backscattered spectra with RPP and RPP+PS. Not only a reduction of the light is observed, but also a reduction of the blue shift and of the width of the spectrum with PS. The laser intensity is 8×10^{13} W/cm².

Another interesting effect is the reduction of the blue shift of the SBS spectra with PS as shown in Fig. 5. Following the discussion of §4, this could indicate a reduction of filamentation of the laser light in the high intensity speckles. It is interesting to notice that such a reduction of the SBS blue shift had been observed in the presence of smoothing by spectral dispersion compared to RPP beam [22]. The SBS and SRS reduction and the change in the SBS shifts that are measured with PS are larger than what was obtained by halving the laser intensity in the RPP beam. The effect of the modification of the intensity distribution with PS is thus amplified by another mechanism such as filamentation. Numerical simulations with parameters close to those of the experiment have shown reduction of self-focusing with PS resulting in a decrease of SBS and SRS gains [20,21].

6. Observation of the Langmuir decay instability

Using masks on both the probe beam and the collecting optics, we selected the scattered light off IAW with wave vectors amplitudes between 2.7 and $3.1xk_0$ (where k_0 is the wave number of the laser light in vacuum). Based on the combined conservation laws of the LDI and SRS decays, these waves correspond to IAW produced by the decay in backward direction of the primary EPW generated by backward SRS within 40°, at an electron density between 10% and 15% of the critical density. IAW propagating in the direction opposite to these IAW and having similar spectral characteristics were simultaneously observed in the Thomson scattered spectra. Such IAW have been predicted theoretically [23]. Numerical simulations have shown that the EPW generated by the first LDI decay may themselves give rise to another LDI decay, producing the so-called LDI cascade [24,25].

A typical spectrum of the Thomson scattered light off IAW is shown in Fig.6. It exhibits the up and down shifted component from the probe frequency, corresponding to light scattered off IAW with wavenumber $\sim 3xk_0$ propagating in opposite directions. By aligning the diagnostic at different locations in the plasma, we observed that the maximum of emission was produced in the front part of the plasma where SRS activity was observed to be the highest. The light off the secondary EPW produced by the Langmuir decay was also observed. A good correlation between the amplitudes of the secondary IAW and the secondary EPW as a function of the primary EPW amplitude was measured, demonstrating that both secondary EPW and IAW were produced by the same Langmuir decay of the primary EPW.

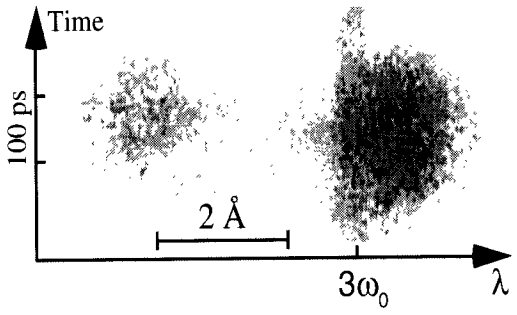

Figure 6 : Time-resolved spectra of up and down Thomson scattered light off ion acoustic waves produced by the Langmuir decay of primary electron plasma waves driven by stimulated Raman scattering and produced by the Langmuir decay of the secondary electron plasma waves .

Theoretical estimates show that self-focusing of the laser light in the speckles should play an important role for laser intensities higher than $6x10^{13}$ W/cm^2, producing high intensity speckles allowing absolute SRS and large density fluctuations. It is then easily shown that the LDI threshold is exceeded for the SRS active speckles. The threshold condition for a secondary LDI decay is very similar to the condition for the primary one starting from SRS and is also satisfied, explaining the observation of subsequent cascades. The clear observation of the LDI instability is important to explain the SRS dependence on ion acoustic waves damping and possible saturation of Raman.

7. Conclusion

Three studies from a LULI experiment have been presented. We have shown that the target composition may influence seriously the levels of SBS and SRS and that a careful understanding of the interaction processes is required to design fusion targets. The observed reduction of SBS and SRS growths with polarization smoothing points out the interest of this technique to control

parametric instabilities. Addition of temporal smoothing can potentially increase the effect. The occurrence of the Langmuir decay instability and the LDI cascade in laser-plasma interaction have been demonstrated by the simultaneous observation of the two LDI products and their subsequent decays. This might explain the dependence of SRS on ion acoustic damping and has interesting application for SRS saturation.

8. Acknowledgments

The authors thank the technical groups of LULI for their aid in the target realization and in the laser operation. The authors gratefully acknowledge the support of W. Seka and the laboratory of Rochester, the participation of B. Canaud and the CEA, of P. Young and S. Glenzer for these experiments, and valuable discussions with D. Berger, B. Cohen, W. Rozmus, G. Bonnaud and E. Lefebvre. Part of this work was performed by the Lawrence Livermore National Laboratory for the U.S. Department of Energy under Contract No. W-7405-ENG-48. Part of this support was provided through the LLNL-LDRD program under the Institute for Laser Science and Applications.

9. References

[1] W. L. Lindl, Phys. Plasmas **2**, 3933 (1995).
[2] W. L. Kruer, *The Physics of Laser plasma Interactions* (Addison Wesley Publishing Co., Redwood City, CA, 1988).
[3] H.A Baldis, E.M. Campbell, and W.L. Kruer, "Laser-plasma interactions", in *Physics of Laser Plasmas,* Handbook of Plasma Physics, North-Holland, Amsterdam 1991, p.361-434.
[4] G. Laval, "La Fusion Thermonucleaire Inertielle par Laser", vol. 1, R. Dautray, J-P Watteau, editors, Eyrolles, Paris (1993).
[5] D. Pesme, "La Fusion Thermonucleaire Inertielle par Laser", vol. 1, R. Dautray, J-P Watteau, editors, Eyrolles, Paris (1993).
[6] W. L. Kruer, S.C. Wilks, B.B. Afeyan, and R.K. Kirkwood, Phys. Plasmas **3**, 382 (1996).
[7] V.V. Eliseev, W. Rozmus, V.T. Tikhonchuk, C.E. Capjack, Phys. Plasmas **3**, 2215 (1996).
[8] D.M. Pennington, M.A. Henasian, S.N. Dixit, H.T. Powell, C.E. Thompson, and T.L. Weiland, Proc. SPIE **1870**, 175 (1993).
[9] Y. Kato, K. Mima, N. Miyanaga, S. Arinaga, Y. Kitagawa, M. Nakatsuka and C. Yamanaka, Phys. Rev. Lett. **53**, 1057 (1984).
[10] S. Skupsky, R.W. Short, T. Kessler, R.S. Craxton, S. Letzring, and J.M. Soures, J. Appl. Phys. **66**, 3456 (1989).
[11] "Phase conversion using distributed polarization rotation", LLE Rev. 45, NTIS Document N°. DOE/DP 40200-149, p.1 (1990) (unpublished).
[12] S. Pau, S.N. Dixit, and Eimerl, J. Opt. Soc. Am. B **11**. 1498 (1994).
[13] K. Tsubakimoto et al., Opt. Comm. **91**, 9 (1992).
[14] J.C. Fernandez, et al., Phys. Rev. Lett. **77**, 2702 (1996) ;
[15] R.K. Kirkwood, et al., Phys. Rev. Lett. **77**, 2706 (1996).
[16] D.S. Montgomery, et al., Phys. Plasmas **5**, 1973 (1998).
[17] C. Labaune, H.A. Baldis, B.S. Bauer, V.T. Tikhonchuk, and G. Laval, Phys. Plasmas 5, 234 (1998).
[18] R.P. Drake and S.H. Batha, Phys. Fluids B **3**, 2936 (1991).
[19] H.A. Baldis and C. Labaune, Rev. Sci. Instr, **67**, 451 (1996).
[20] R.L. Berger, E. Lefebvre, A.B. Langdon, J.E. Rothenberg, C.H. Still, and E.A. Williams, Phys. Plasmas **6**, 1043 (1999).
[21] S. Hüller, Ph. Mounaix, V.T. Tikhonchuk, Phys. Plasmas **5**, 2706 (1998).
[22] J.D. Moody, et al., Phys. Plasmas **2**, 4285 (1995).
[23] D.F. DuBois, H.A. Rose, and D.A. Russel, Phys. Rev. Lett. **66**, 1970 (1991).
[24] T. Kolber, W. Rozmus, and V.T. Tikhonchuk, Phys. Fluids B **5**, 138 (1993).

[25] D.A. Russel, D. F. DuBois and H. A. Rose, Phys. Plasmas **6**, 1294 (1999).